Mem. S.A.It. Vol. 87, 513

Memorie della

N-body simulations with BSSs: defining mass segregation indicators

E. Alessandrini, on behalf of the Cosmic-Lab team

Dept. of Physics and Astronomy, University of Bologna, Viale Berti Pichat, 6/2
e-mail: emilian.alessandrini@unibo.it

Abstract. Blue Straggler stars (BSSs) are proven tools to measure the level of mass segregation and the dynamical age of globular clusters (GCs). In order to study the segregation process of BSSs as a function of time, we are performing N-body simulations of GCs also including a population of massive stellar remnants. In this context we have defined a new indicator of mass segregation based on the comparison between the cumulative BSS radial distribution and that of a reference population. Preliminary results are shown.

Key words. globular clusters: general – Stars: kinematics and dynamics – Methods: numerical

1. Introduction

During the last twenty years, many observational studies directed to sample the radial distribution of Blue Straggler Stars (BSSs) in globular clusters (GCs) have been carried out (e.g., Ferraro et al. 1993, 1997, 2004, 2006, 2009; Lanzoni et al. 2007a,b,c; Dalessandro et al. 2008a,b, 2013; Beccari et al. 2011). According to these studies, different shapes of the BSS radial distribution have been found, suggesting different level of mass segregation in GCs. Recently Ferraro et al. (2012) proposed to use the shape of the normalized BSS radial distribution[1] as an indicator of the level of dynamical evolution experienced by a stellar system, grouping GCs in three main families (*Family I, II* and *III*) of increasing dynamical ages. In this scenario, dynamical friction (DF) is the main phenomenon that drives the BSS sedimentation toward the cluster center, modifying an initially flat BSS radial distribution (*Family I* GCs), into a bimodal distribution, with a central peak, a minimum and an outer rising branch (*Family II*), and eventually leading to a unimodal BSS distribution, that monotonically decreases outward (*Family III*). Theoretical confirmations of this result have been searched by means of semi-analytic and numerical approaches (Alessandrini et al. 2014; Miocchi et al. 2015), providing some additional support to the observations. However, these works seem to suffer from an insufficient level of realism, as an insufficiently large number of particles ($N = 10^4$) and no populations of dark remnants (DRs), such as neutron stars (NSs) and stellar mass black holes (BHs).

For a more appropriate interpretation of the observational results, in the present work we discuss a set of more realistic N-body simulations that include

(i) $N \simeq 10^5$ particles,

[1] With "normalized BSS distribution" here we indicate the double normalized ratio defined in Ferraro et al. (1993).

(ii) a mass-spectrum obtained from the evolution of a Kroupa (2001) Initial Mass Function (IMF),

(iii) a population of heavy DRs.

2. N-body simulations

The simulations exploit the Graphic Processing Unit (GPU) version of the direct N-body code `NBODY6` (Nitadori & Aarseth 2012) on the `BIGRED2` supercomputer at Indiana University, Bloomington.

The initial conditions have been built as follows: starting from 99700 stars belonging to a Kroupa (2001) IMF, in the mass interval $m = [0.1, 100]M_\odot$ and assuming a metallicity $Z = 0.001$, we evolved the system for 12 Gyr, using the stellar evolution recipes implemented in the SSE version of the software `McLuster` (Hurley et al. 2000, 2002; Küpper et al. 2011). This procedure generated a population of white dwarfs and DRs descending from the evolution of stars with initial masses $m > 0.8M_\odot$. Then, we assumed two different DR retention fractions, $f_{\rm DR} = 10\%$ and 30%, meaning that 90% and 70%, respectively, of the total number of NSs and BHs generated from the evolution of the IMF have been excluded from the simulations. For the sake of comparison, we also explored a third case with no DRs, where the 99700 stars have masses within the interval $[m = 0.1, 0.8]M_\odot$ distributed following the adopted IMF. To all the runs we also added 300 BSSs, modeled as single particles with a mass of $1.2M_\odot$.

We assumed the particles follow a King (1966) model distribution with no primordial mass segregation. In order to explore the effect of different concentrations, we have chosen two different values of the King central dimensionless potential: $W_0 = 5$ and $W_0 = 8$. We therefore ran a total of six simulations, named with the notation $S^{W_0}_{f_{\rm DR}}$.

3. Results

Fig. 1 shows the evolution of the 5%, 10% and 50% number Lagrangian radii of particles belonging to different populations in the simulation $W_0 = 8$. We compare the evolution of the Lagrangian radii of BSSs (blue lines), of what we call *reference* population (REF), corresponding to all the particles with masses between 0.75 and 0.84 $M_\odot$ (red lines), and of the overall system, including all particles of any mass (grey lines). For the runs with DRs, we also show in black the evolution of the DR population. The figure clearly shows that the cluster dynamical evolution is highly affected by the presence and the amount of DRs. If no DRs are present (left-hand column), BSSs drive the cluster toward core collapse (CC), because they are the most massive objects within the system. In the S^8_{10} and even more in the S^8_{30} simulation, instead, DRs undergo a rapid decoupling from the other populations, forming a subsystem that quickly sinks toward the centre (see the black curves in the central and right columns of Fig. 1). This behaviour has been found and discussed also by Sigurdsson & Hernquist (1993), Kulkarni et al. (1993), and very recently by Banerjee et al. (2010) and Breen & Heggie (2013b). The overall system reacts with a continuos expansion of r_{50} (grey

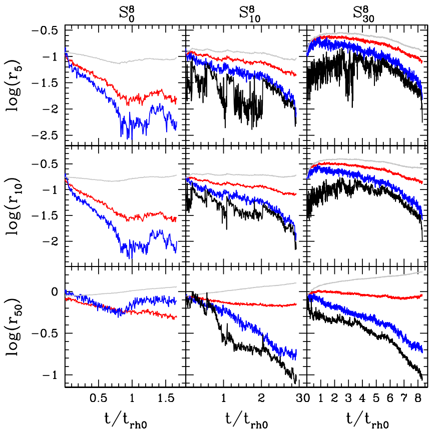

Fig. 1. Evolution of the Lagrangian radii containing 5%, 10% and 50% (top, central and bottom panels, respectively) of the relative number of DRs (black), BSSs (blue), REF stars (red), and particles of any mass (grey), for the three runs with $W_0 = 8$. Time is normalized to the initial half-mass relaxation time $t_{\rm rh0}$ of each run.

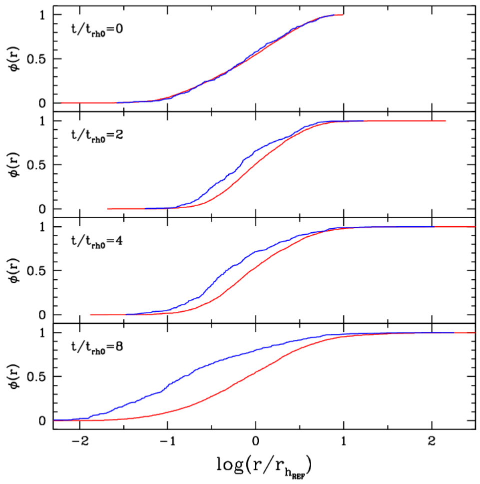

Fig. 2. From top to bottom, time evolution of the cumulative radial distributions of BSSs (blue lines) and REF stars (red lines), for the S_{30}^{8} simulation. The radial scale is logarithmic, with the radius normalized to the half-mass radius of the REF population measured at any considered evolutionary time (see labels).

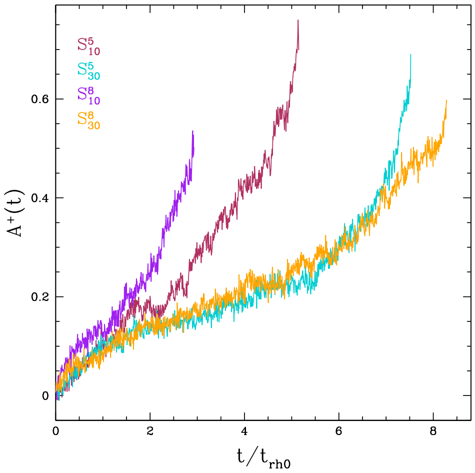

Fig. 3. Time evolution of A^+ in the four simulations with DRs (see labels).

lines in the bottom central and right panels). Hence, according to what expected, DRs (especially stellar-mass BHs, which are the most massive objects in the system) play a fundamental role in cluster dynamics, driving the CC of the visible component, determining its timescale and inhibiting the central segregation of BSSs. In the rest of our discussion, we focus our attention on the simulations including DRs.

3.1. Cumulative radial distributions

Many previous studies have shown that the BSS cumulative radial distributions, $\phi(r)$, vary from cluster to cluster (e.g., Ferraro et al. 2003; Mapelli et al. 2004, 2006). By using our N-body simulations, here we study how the cumulative radial distributions of BSSs and REFs depend on the simulated cluster properties. Since in all runs we assume no initial mass segregation, at $t = 0$ the two distributions are superimposed. As time increases, BSSs migrate toward the cluster centre more rapidly than the REF population and the two corresponding cumulative radial distributions start to separate, the one of BSSs becoming steeper than the other.

This process is evident in Fig. 2, which shows the cumulative radial distributions of BSSs and REFs (blue and red lines, respectively) for the S_8^{30} run, at four different evolutionary times: at $t = 0$ the two populations are perfectly mixed and their cumulative radial distributions superimposed; then, for increasing time, the two distributions become more and more separated due to the effect of DF on BSSs. The same qualitative trend is observed in all simulations, suggesting that the separation between the two cumulative distributions can be used to measure the level of BSS central segregation. Hence, we quantitatively define a new indicator, A^+, as the area between the BSS and the REF cumulative radial distributions in the $\phi(r) - \log(r/rh_{\mathrm{REF}})$ plane (with rh_{REF} being the half-mass radius of the REF population).

Fig. 3 shows the time dependence of A^+ in our simulations and confirms that this parameter is a sensitive indicator of the BSS sedimentation process, always increasing with time. Fig. 3 also shows that the time dependence of A^+ is characterized by two main regimes: an initial, slower phase, followed by a steeper trend toward the end of the simulations, at times approaching the CC time of the visible component. This fact demonstrates that A^+ is an indicator both of the level of BSS segregation and of the whole dynamical evolution of the system. We see that toward the end of all the runs, A^+ assumes comparable values, suggesting that this parameter might be used also to guess whether a cluster is close to the CC phase of its visible component, independently of its concentration and DR fraction. A larger exploration of the parameter space is needed before drawing more quantitative conclusions. On the observational side, a forthcoming paper will be devoted to the empirical determination of A^+ for a sample of Galactic GCs and to the study of the observational correlations between this parameter and other possible indicators of cluster dynamical evolution.

Acknowledgements. The author thanks the *Marco Polo Project* of the Bologna University and the Indiana University for the hospitality during his stay in Bloomington, where part of this work was carried out thanks to the computer cluster BigRed2, one of the technology facility of IU.

References

Alessandrini, E., et al. 2014, ApJ, 795, 169

Banerjee, S., Baumgardt, H., Kroupa, P. 2010, MNRAS, 402, 371

Beccari, G., et al. 2011, ApJ, 737, 3

Breen, P. G., Heggie, D. 2013b, MNRAS, 436, 584

Dalessandro, E., et al. 2008, ApJ, 681, 311

Dalessandro, E., Lanzoni, B., Ferraro, F. R., et al. 2008a, ApJ, 677, 1069

Dalessandro, E., Lanzoni, B., Ferraro, F. R., et al. 2008b, ApJ, 681, 311

Dalessandro, E., Ferraro, F. R., Massari, D., et al. 2013, ApJ, 778, 135

Ferraro, F. R., Pecci, F. F., Cacciari, C., et al. 1993, AJ, 106, 2324

Ferraro, F. R., Paltrinieri, B., Fusi Pecci, F., et al. 1997, A&A, 324, 915

Ferraro, F. R., et al. 2003, ApJ, 588, 464

Ferraro, F. R., Beccari, G., Rood, R. T., et al. 2004, ApJ, 603, 127

Ferraro, F. R., Sollima, A., Rood, R. T., et al. 2006, ApJ, 638, 433

Ferraro, F. R., Beccari, G., Dalessandro, E., et al. 2009, Nature, 462, 1028

Ferraro, F. R., Lanzoni, B., Dalessandro, E., et al. 2012, Nature, 492, 393

Hurley, J. R., Pols, O. R., Tout, C. A. 2000, MNRAS, 315, 543

Hurley, J. R., Pols, O. R., Tout, C. A. 2002, MNRAS, 329, 897

King, I. R. 1966, AJ, 71, 64

Kroupa, P. 2001, MNRAS, 322, 231

Küpper, A. H. W., et al. 2011, MNRAS, 417, 2300

Kulkarni, S. R., Hut, P., McMillan, S. 1993, Nature, 364, 421

Lanzoni, B., Dalessandro, E., Perina, S., et al. 2007a, ApJ, 670, 1065

Lanzoni, B., Sanna, N., Ferraro, F. R., et al. 2007b, ApJ, 663, 1040

Lanzoni, B., Dalessandro, E., Ferraro, F. R., et al. 2007c, ApJ, 663, 267

Mapelli, M., et al. 2004, ApJ, 605, L29

Mapelli, M., et al. 2006, MNRAS, 373, 361

Miocchi, P., et al. 2015, ApJ, 799, 44

Nitadori, K., & Aarseth, S. J. 2012, MNRAS, 424, 545

Sigurdsson, S., Hernquist, L. 1993, Nature, 364, 423